

Density Functional Theory Studies of $[\text{Fe}(\text{O})_2\text{L}]^{2+}$: What is the Role of the Spectator Ligand L with Different Coordination Numbers?

Glenna So Ming Tong^{*[a]} and Chi-Ming Che^{*[a]}

Keywords: Density functional calculations / Iron / High-valency / Oxido ligands / Amines

Density functional theory (DFT) studies were carried out on $[\text{Fe}(\text{O})_2(\text{L})]^{n+}$ [$\text{L} = \text{qpy}$ (**1**), simple amines (**2**), and tpy (**3**); $\text{qpy} = 2,2':6',2'':6'',2''':6''',2''''$ -quinquepyridine and $\text{tpy} = \text{terpyridine}$; $n = 1$ or 2] to study how the coordination number of the spectator ligand L affects the geometries and electronic structures of the complexes. It was found that qpy can act as both a tridentate and pentadentate ligand resulting in $[\text{Fe}(\text{O})_2(\text{qpy})]^{2+}$ (**1**²⁺) having a trigonal bipyramidal (TBP) geometry in the former case, and a pentagonal bipyramidal (PBP) geometry in the latter case. The difference in coordination geometries has a significant impact on the electronic structures of **1**²⁺. With a TBP geometry, **1**²⁺ adopts a $[\text{Fe}^{\text{V}}(\text{O})_2(\text{qpy})^{+}]^{2+}$ formalism where a d³ quartet Fe^{V} ion ferromagnetically and antiferromagnetically couples to the qpy cation radical to give close-lying triplet and quintet states (within ca. 0.2 eV). With a PBP geometry, the Fe^{V} ion in **1**²⁺ also formally has

three unpaired electrons (a d³ quartet) with the fourth unpaired electron localized on a single oxido ligand to give a quintet state. The unoccupied orbital of **1**²⁺ in PBP geometry is lower lying in energy and has higher oxido character than when the complex has TBP geometry. Thus, based on the MO energies and oxido character of the unoccupied orbital, **1**²⁺ with PBP geometry is proposed to be a more reactive oxidant than **1**²⁺ with TBP geometry. On the other hand, **1**²⁺ with TBP geometry has a similar electronic structure to heme Cpd I, and it is possible that these two compounds have similar oxygen atom transfer reaction mechanisms. By varying the ligand coordination number using different spectator ligands L, the dioxido-iron complex $[\text{Fe}(\text{O})_2(\text{L})]^{2+}$ can change from a high-spin triplet when $\text{L} = \text{tpy}$, to a low-spin singlet when $\text{L} = \text{simple amines}$, to a quasi-degenerate triplet and quintet state when $\text{L} = \text{qpy}$.

Introduction

Oxido-iron complexes have been one of the most pursued types of compounds in chemistry. This is partly due to their relevance in bio-catalytic transformations^[1–7] and potential use as green oxidants.^[8–10] The literature shows that much effort has been devoted to the study of six-coordinate monooxido-iron(IV) and -(V) complexes as these species are postulated to be key reaction intermediates in biological and synthetic biomimetic systems.^[7,11,12] Only a few studies of monooxido-iron complexes with coordination numbers other than six have been reported. Bollinger, Neese, and Krebs combined spectroscopic and DFT approaches to deduce the structural details of the C–H bond activation step(s) in the TauD reaction cycle.^[13] In addition to the six-coordinate octahedral (Oh) model, five-coordinate trigonal bipyramidal (TBP) and square pyramidal (SP) models have also been considered as reactive $\text{Fe}^{\text{IV}}=\text{O}$ intermediates.^[13] It was found that the calculated spectroscopic parameters of iron(IV)-oxido reaction intermediates are inconsistent with

experimental data when an SP model is adopted, but in agreement with the experimental values if either an Oh or a TBP mode is applied. Que, Bominaar, Münck, and Collins reported the five-coordinate $[\text{Fe}^{\text{V}}(\text{O})(\text{TAML})]^-$ (TAML = tetraamido macrocyclic ligand) complex with a SP geometry; this complex is capable of oxidizing triphenylphosphane, thioanisole, styrene and cyclooctene to give the corresponding oxides, performing C–H bond hydroxylation of ethylbenzene to give a mixture of 1-phenylethanol and acetophenone, and oxidizing 9,10-dihydroanthracene to give anthracene.^[14] Studies of dioxido-iron complexes are sparse compared to their 2nd and 3rd row analogues. We have recently detected a dioxido-iron complex, $[\text{Fe}(\text{O})_2(\text{qpy})]^{2+}$, generated from the oxidation of $[\text{Fe}(\text{qpy})(\text{MeCN})_2]^{2+}$ by Oxone in MeCN under ESI-MS conditions.^[15] Notably, we found that 5 mol-% of $[\text{Fe}(\text{qpy})(\text{MeCN})_2]^{2+}$ catalyzed the oxidation of cyclohexane by Oxone to give a mixture of cyclohexanol and cyclohexanone with turnovers of 8 and 3.2, respectively; this reaction was performed in MeCN for a period of 2 h at room temperature.^[16] We hypothesize that $[\text{Fe}(\text{O})_2(\text{qpy})]^{2+}$ is probably a key reaction intermediate as related monooxido-iron(IV) complexes, such as $[\text{Fe}(\text{Cl}_3\text{terpy})_2\text{O}]^{2+}$ generated in situ by the oxidation of $[\text{Fe}(\text{Cl}_3\text{terpy})_2]^{2+}$ by Oxone, is not reactive towards the oxidation of cyclohexane under similar experimental conditions.^[17] In silico, we have found that *trans*- $[\text{Fe}(\text{O})_2(\text{NH}_3)_2(\text{NMeH}_2)_2]^{2+}$ could be a stable entity.^[15] Subsequently,

[a] Department of Chemistry and Open Laboratory of Chemical Biology of the Institute of Molecular Technology for Drug Discovery and Synthesis, The University of Hong Kong, Pokfulam Road, Hong Kong
E-mail: tongsm@hku.hk
cmche@hku.hk

Supporting information for this article is available on the WWW under <http://dx.doi.org/10.1002/ejic.201000656>.

Münck and Que suggested the possible existence of a *trans*-dioxido-iron(VI) species, $[\text{Fe}(\text{O})_2(\text{TMC})]^{2+}$ (TMC = 1,4,8,11-tetramethyl-1,4,8,11-tetraazacyclotetradecane); their rationale was based on this complex's higher oxidizing power compared to $[\text{Fe}(\text{O})(\text{TMC})(\text{NCMe})]^{2+}$ and drawing an analogy with a ruthenium counterpart.^[18] High-valent dioxido metal complexes are of interest because four oxidizing equivalents could be transferred to a substrate with one equiv. of dioxido metal complex, and when the oxido units are displaced in a *cis*-fashion, 1,2-dihydroxylation of alkenes could be possible.

The ligand qpy has five pyridyl rings and, in principle, acts as a pentadentate ligand. As such, $[\text{Fe}(\text{O})_2(\text{qpy})]^{2+}$ ($\mathbf{1}^{2+}$) could adopt a seven-coordinate geometry similar to its precursor, $[\text{Fe}(\text{qpy})(\text{NCMe})_2]^{2+}$, with qpy occupying the equatorial plane (**1a**, see Scheme 1).^[19] Thus, this dioxido complex should have pseudo- C_5 symmetry and the d-orbitals should split in a 2–2–1 manner. The e_2 pair $\text{Fe}(\text{d}_{xy}, \text{d}_{x^2-y^2})$ is lowest in energy, followed by the e_1 pair, which are an antibonding combination of $\text{Fe}(\text{d}_{xz}, \text{d}_{yz})$ and $\text{O}(\text{p}_x, \text{p}_y)$ orbitals ($\pi^*(\text{Fe}-\text{O})$). The a -type orbital, being an antibonding combination of $\text{Fe}(\text{d}_{z^2})$ and $\text{O}(\text{p}_z)$ orbitals ($\sigma^*(\text{Fe}-\text{O})$), is highest in energy (the z -axis is set along the $\text{O}-\text{Fe}-\text{O}$ bond). With this electronic configuration the ground state of $\mathbf{1}^{2+}$ is a triplet ($S = 1$) with the two electrons singly occupying the e_2 orbitals. In contrast, the ground state of six-coordinate *trans*- $[\text{Fe}(\text{O})_2(\text{NH}_3)_2(\text{NMeH}_2)_2]^{2+}$ ($\mathbf{2}^{2+}$) is a singlet ($S = 0$) with the two electrons doubly occupying the d_{xy} orbital (see Scheme 2). The difference in the ground state electronic structures for these two species could have a significant impact on their reactivity. For instance, the first step of C–H or C=C bond activation involves the electron in the donor orbital (ϕ_{CH} or ϕ_{CC}) going into the π^* ($\text{Fe}-\text{O}$) orbitals. As this π^* orbital does not involve the equatorial ligand, its orbital energy should be similar for the two complexes, therefore the activation barrier for this first step should also be similar for $\mathbf{1}^{2+}$ and $\mathbf{2}^{2+}$ based on their ground state orbitals. However, for the rebound step the second electron of the ϕ_{CH} (or ϕ_{CC}) orbital has to go into a $\pi^*(\text{Fe}-\text{O})$ orbital in the case of $\mathbf{2}^{2+}$, whereas for $\mathbf{1}^{2+}$ the electron can go into the nonbonding e_2 orbital and this electron transfer step requires no activation unlike the rebound step that occurs in complex $\mathbf{2}^{2+}$. Thus, C–H hydroxylation and C=C epoxidation should be faster with $\mathbf{1}^{2+}$ than with $\mathbf{2}^{2+}$. Therefore, it

is of interest to study the electronic structures and spin state energetics of $\mathbf{1}^{2+}$. To our surprise, the lowest energy structure of $\mathbf{1}^{2+}$ is not a seven-coordinate structure but a five-coordinate one with qpy acting as a tridentate ligand, and the $\text{O}-\text{Fe}-\text{O}$ angle being ca. 120° instead of linear as in the proposed seven-coordinate structure (see **1c**, Scheme 1).

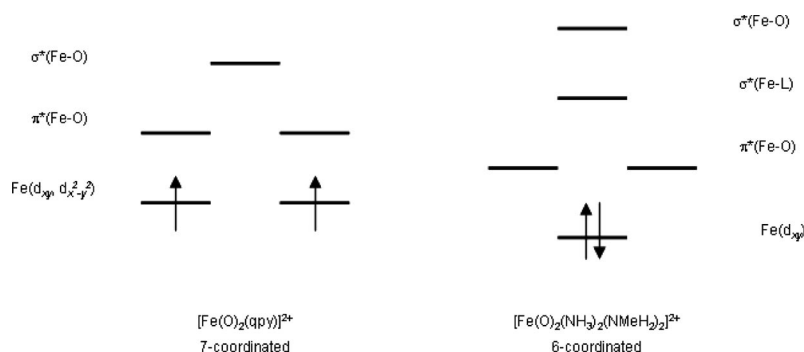


Scheme 1. Geometries of complexes $\mathbf{1}^{2+}$.

Why does $[\text{Fe}(\text{O})_2(\text{qpy})]^{2+}$ energetically prefer a five-coordinate structure instead of a seven-coordinate one? In the present work, we performed density functional theory (DFT) calculations to examine the electronic structures and spin state energetics of $\mathbf{1}^{2+}$. In addition, we have also carried out similar calculations on $[\text{Fe}(\text{O})_2(\text{tpy})]^{2+}$ ($\mathbf{3}^{2+}$, tpy = terpyridine) in which the two dangling pyridyl rings of $\mathbf{1}^{2+}$ in its TBP geometry were removed. Comparisons of the electronic structures of $\mathbf{1}^{2+}$ with that from our previous calculations on $\mathbf{2}^{2+}$ ^[15] were also made.

Results

In what follows, we individually present the calculation results for complexes $\mathbf{1}^{n+}$ – $\mathbf{3}^{n+}$. The geometries, relative spin state energetics, and electronic structures of the complexes for $n = 2$ with $S = 0, 1$, and 2 will be given first followed by those for $n = 1$ with $S = 1/2$ and $3/2$. The electron affinities (EA) of the dipositive ions $\mathbf{1}^{2+}$ – $\mathbf{3}^{2+}$ were calculated with and without solvent included in the model. In general, the relative energies from UOLYP single-point calculations using a large basis set, BS2, agree well with those obtained



Scheme 2.

using a smaller basis set, BS1 (see computational details). Hence, the data depicted below will be those from the UOLYP/BS1 calculations unless otherwise specified.

Hereafter, when the notation \mathbf{X}^{n+} (where $\mathbf{X} = \mathbf{1}, \mathbf{2}$, and $\mathbf{3}$ and $n = 1$ or 2) is used without a preceding superscript to define the spin state of the complex, it refers to the general form of the complexes i.e. no consideration has been given to the spin states and geometries of the complexes.

1. $[\text{Fe}(\text{O})_2(\text{qpy})]^{n+}$ (**1**)

A. Optimized geometries and relative energies of the different spin states of $\mathbf{1}^{2+}$. The optimized geometries and relative energies of $\mathbf{1}^{2+}$ in different spin states are listed in Table S1. Geometry optimization of $\mathbf{1}^{2+}$ led to three local minimum energy structures for the triplet and quintet states: $\mathbf{1a}^{2+}$ with PBP geometry, and $\mathbf{1b}^{2+}$ and $\mathbf{1c}^{2+}$ with TBP geometry. Conformers $\mathbf{1c}^{2+}$ and $\mathbf{1b}^{2+}$ differ only in the orientations of the dangling pyridyl rings: $\mathbf{1b}^{2+}$ has the 4th and 5th pyridyl rings moved toward the z-axis while $\mathbf{1c}^{2+}$ has these two pyridyl rings moved away from the z-axis (see Scheme 1 and the Supporting Information). Conformer $\mathbf{1c}^{2+}$ is found to be slightly more stable than $\mathbf{1b}^{2+}$ (ca. 0.12 eV for the triplet state and ca. 0.04 eV for the quintet state), so only the results for $\mathbf{1c}^{2+}$ are presented for the TBP geometry unless otherwise stated.

The lowest energy state of $\mathbf{1}^{2+}$ is $^3\mathbf{1c}^{2+}$ with $^5\mathbf{1c}^{2+}$ ca. 0.17 eV higher in energy. The results from the UOLYP/BS1 calculations show that the $^{3,5}\mathbf{1a}^{2+}$ states are ca. 0.8 and 0.98 eV higher in energy than $^3\mathbf{1c}^{2+}$, respectively. However, single-point energy calculations at the OLYP-optimized geometries using B3LYP predict that the lowest energy state is $^5\mathbf{1a}^{2+}$, ca. 0.18 eV lower in energy than the TBP $^{3,5}\mathbf{1c}^{2+}$ structure. It should be noted that hybrid density functional calculations are well-known to be biased towards high-spin states,^[20] and $^5\mathbf{1a}^{2+}$ has the highest spin density on Fe ($\rho_{\text{Fe}} = 2.81$) amongst the spin states and structures studied (see Table S7 in the Supporting Information). Thus, the B3LYP calculations may overestimate the d-d exchange stabilization. The singlet state lies at ca. 0.44 eV higher in energy than $^3\mathbf{1c}^{2+}$. Hence, $\mathbf{1}^{2+}$ prefers a five-coordinate TBP geometry over a seven-coordinate pentagonal bipyramidal (PBP) geometry according to the OLYP results.

The Fe–O bond lengths in $\mathbf{1}^{2+}$ with TBP geometry are rather short, and are in the range of 1.596–1.615 Å irrespective of the spin state being a singlet, triplet or quintet, on the other hand, for $^{3,5}\mathbf{1a}^{2+}$ with a PBP geometry the Fe–O distances span a wider range of 1.614–1.763 Å. Interestingly, for $\mathbf{1c}^{2+}$, the O–Fe–O unit is not disposed symmetrically about the plane defined by the three pyridyl rings coordinated to Fe. The two N2–Fe–O angles are ca. 104° and 140° for the triplet states and ca. 100° and 142° for the quintet states (N2 is the nitrogen atom of py2, the 2nd pyridyl ring of the qpy ligand). Conversely, for $^1\mathbf{1}^{2+}$, the O–Fe–O unit is almost symmetrically disposed about the plane defined by py1–py3 (N2–Fe–O1/O2 angles: 125/116°). For $^{3,5}\mathbf{1a}^{2+}$ the O–Fe–O angle is essentially linear (176 and 172° for the triplet and quintet states, respectively).

B. Electronic structures of $\mathbf{1}^{2+}$ in different spin states.

What is the difference between the electronic structures of $\mathbf{1}^{2+}$ in TBP and PBP geometries? Figure 1 shows the MO diagram for $^3\mathbf{1c}^{2+}$ (For MOs of $^{3,5}\mathbf{1b}^{2+}$ and $^5\mathbf{1c}^{2+}$ see the Supporting Information). The lowest energy orbital is derived from the antibonding combination of Fe(d_{xy}) and O(p_x) orbitals, and the second lowest is formed by the antibonding combination of Fe(d_{xz}) and O(p_x) orbitals. The third lowest lying orbital involves the antibonding combination of a mixture of Fe(d_{yz} , $d_{x^2-y^2}$) and O(p_y) orbitals. These three lowest lying orbitals are π^* in nature. The two highest lying MOs involve the antibonding combination of Fe(d_{z^2}) and O(p_z) orbitals and the antibonding combination of Fe($d_{x^2-y^2}$, d_{yz}) and O(p_y) orbitals. These two MOs have mixed σ^*/π^* character, a consequence of the asymmetric disposition of the oxido ligands relative to the py1–py3 plane. There is also a low lying qpy-based ligand orbital, denoted qpy(σ^*), which is key to the electronic structures of the $^{3,5}\mathbf{1c}^{2+}$ states. The three lowest lying $\pi^*(\text{Fe–O})$ orbitals are singly occupied in the $^{3,5}\mathbf{1c}^{2+}$ states, leaving the two highest lying $\sigma^*/\pi^*(\text{Fe–O})$ orbitals vacant. The low lying qpy(σ^*) orbital is also singly occupied and the spin direction of the electron occupying this orbital determines whether the state is a triplet or a quintet: if it is antiferromagnetically coupled to the $\pi^*(\text{Fe–O})$ electrons it is a triplet state, if it is ferromagnetically coupled it is a quintet state. As such, the $^{3,5}\mathbf{1c}^{2+}$ states are best described as a quartet $\text{Fe}^{\text{V}}(\text{O})_2$ moiety coupled with a qpy cation radical, $[\text{Fe}^{\text{V}}(\text{O})_2(\text{qpy}^+)]^{2+}$ (see the spin densities given in Table S7 in the Supporting Information). This MO picture closely corresponds to that of the Cpd I iron(IV)-oxido Heme system, where the triplet $\text{Fe}^{\text{IV}}\text{–O}$ moiety antiferromagnetically or ferromagnetically couples to the porphyrin cation radical to give a doublet or quartet state, respectively.^[21]

For $\mathbf{1a}^{2+}$ with a seven-coordinate PBP geometry only the quintet state is described here, for there is severe spin-contamination in the case of $^3\mathbf{1a}^{2+}$ ($S^2 = 2.48$, which is a deviation from the ideal value of 2.00, while $^5\mathbf{1a}^{2+}$ has $S^2 = 6.04$, which is only slightly deviated from the ideal value of 6.00). There may be two reasons for the significant spin contamination for the triplet state: (1) the optimized geometries are a mixture of microstates derived from higher spin states, i.e., they are made up of the triplet components of the quintet, septet, etc states besides the “genuine” triplet state ($S^2 = 2$ and $S_z = 1$); (2) the triplet state is multi-configurational such that it cannot be described by a simple MO picture of a single determinant.

Figure 2 presents the MO diagram of $^5\mathbf{1a}^{2+}$. Considering the d-block orbitals, the lowest lying α -spins involve the σ -antibonding combination of Fe(d_{xy} , $d_{x^2-y^2}$) and qpy orbitals with the d_{xy} orbital ca. 0.3 eV lower in energy. This is followed by the Fe(d_{xz} , d_{yz}) pair interacting with the O1(p_x , p_y) orbitals in a π^* -fashion. The σ -antibonding combination between Fe(d_{z^2}) and the O(p_z) orbitals lies highest in energy. For the β -spins, the frontier MOs involving d-orbitals are similar in energy, but with Fe($d_{x^2-y^2}$) ca. 0.2 eV higher in energy than the Fe(d_{xz} , d_{yz}) orbitals, with the latter mixed with some d_{xy} character. Note that for the α -spins the π^*

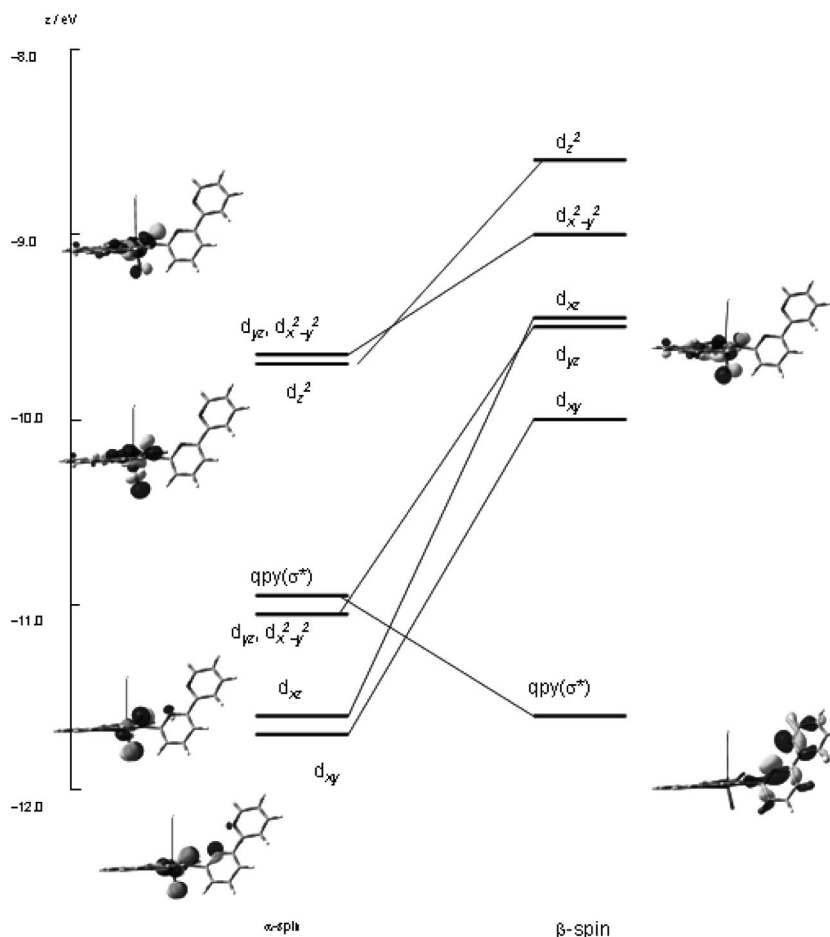


Figure 1. MO diagram for ${}^3\mathbf{1c}^{2+}$.

combination between the $\text{Fe}(d_{xz}, d_{yz})$ and $\text{O}(p_x, p_y)$ orbitals gives rise to an orbital mainly localized on O1, whereas for the β -spins the corresponding interaction leads to an orbital mainly localized on O2. In addition, there are two low lying occupied MOs with significant O1/O2 contributions that have different compositions in the α - and β -spin states: α -MO111 and α -MO112 are mainly of $\text{O2}(p_y)$ and $\text{O2}(p_x)$ character, whereas for β -MO112 and β -MO115 (β -LUMO) there are additional contributions from $\text{O1}(p_x, p_y)$. The difference in MO compositions between the α - and β -spins may be a result of spin polarizations. For ${}^5\mathbf{1a}^{2+}$ the first three lowest lying d-orbitals are singly occupied such that the Fe center could be described as Fe^{V} , with some spin density delocalized onto the qpy ligand. Moreover, due to spin polarizations, the O1 atom has partial negative spin density (see Table S7 in the Supporting Information for the spin density values).

C. Optimized geometries, relative energies, and electronic structures for the different spin states of $\mathbf{1}^+$. Upon one-electron reduction of $\mathbf{1}^{2+}$ to give $[\text{Fe}(\text{O})_2(\text{qpy})]^+$, there are one and two local minima for the doublet and quartet states, respectively.

The optimized doublet state, denoted as ${}^2\mathbf{1}^+$, has geometry similar to that of ${}^1\mathbf{1}^{2+}$, with slightly elongated Fe–O dis-

tances (1.609–1.615 Å). The O–Fe–O unit is also nearly symmetrically disposed about the plane defined by py1–py3. However, the py4 and py5 rings are displaced away from the z-axis, as also observed for ${}^{3,5}\mathbf{1c}^{2+}$. For ${}^1\mathbf{1}^{2+}$ two electrons doubly occupy the lowest lying $\pi^*(\text{Fe}(d_{xy})-\text{O}(p_x))$ orbital, and hence ${}^1\mathbf{1}^{2+}$ could be described as $[\text{Fe}^{\text{VI}}(\text{O})_2(\text{qpy})]^{2+}$ (see Supporting information). The additional electron thus goes into the LUMO of the singlet state, which is a $\pi^*(\text{Fe}(d_{xz})-\text{O}(p_x))$ orbital to give ${}^2\mathbf{1}^+$, and hence causes the elongation of the Fe–O bonds. This state is thus best described as $[\text{Fe}^{\text{V}}(\text{O})_2(\text{qpy})]^+$.

For the quartet states the lowest energy is ${}^4\mathbf{1b}^+$. This is actually the lowest energy state amongst the optimized spin states of $\mathbf{1}^+$ (ca. 0.30 eV below ${}^2\mathbf{1}^+$). In this state the Fe–O distances are similar to that of ${}^{3,5}\mathbf{1b}^{2+}$, with Fe–N4 and Fe–N5 distances in between those values observed for ${}^3\mathbf{1b}^{2+}$ and ${}^5\mathbf{1b}^{2+}$. The O–Fe–O moiety is also asymmetrically disposed about the py1–py3 plane (see Table S1 in the Supporting Information). It is not surprising that the geometries of the O–Fe–O units of ${}^4\mathbf{1b}^+$ and ${}^{3,5}\mathbf{1b}^{2+}$ are similar, because the extra electron of the former is added to the qpy ligand ($\text{qpy}(\sigma^*)$ orbital). Therefore, ${}^4\mathbf{1b}^+$ could also be described as $[\text{Fe}^{\text{V}}(\text{O})(\text{qpy})]^+$, analogous to the Cpd 0 iron(IV)-oxido of the heme systems. As the spin densities

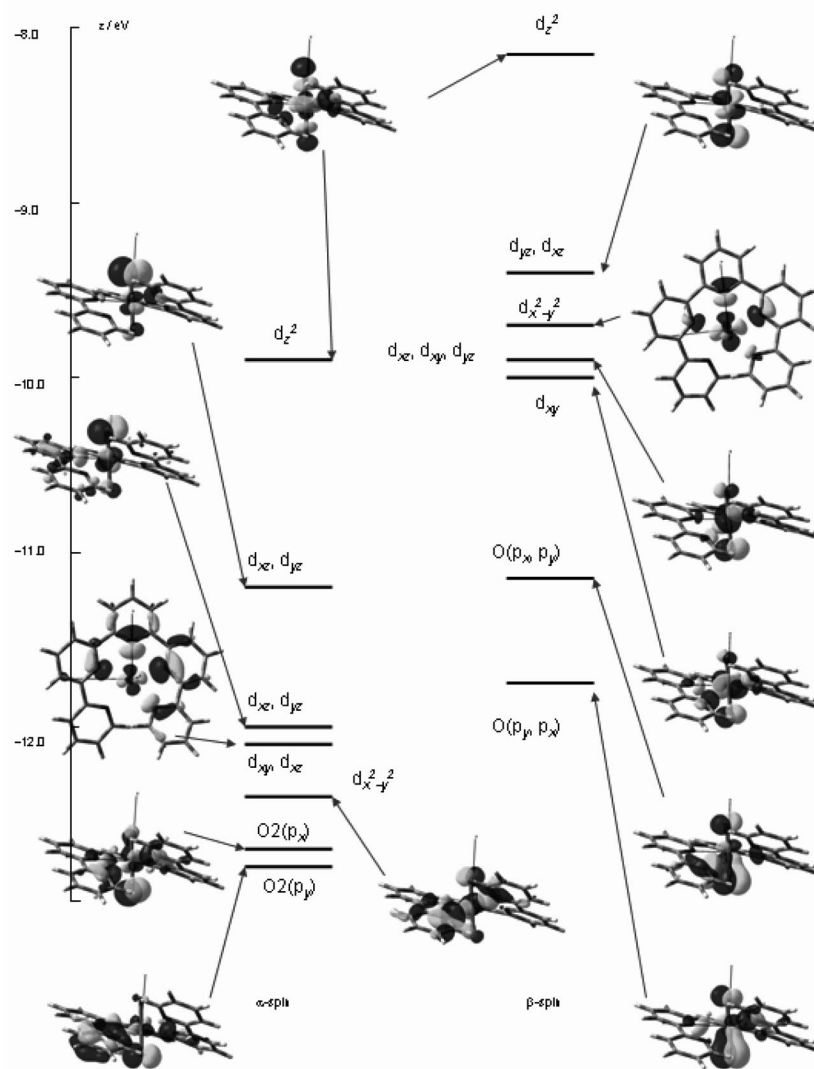


Figure 2. MO diagram for ${}^5\mathbf{1a}^{2+}$.

on Fe for both the quartet and quintet states are similar, ${}^4\mathbf{1b}^+$ could also be described as a Fe^{V} complex (see Table S7 in the Supporting Information).

${}^4\mathbf{1a}^+$ has geometry similar to that of ${}^{3,5}\mathbf{1a}^{2+}$, and according to the UOLYP/BS1 calculations, is ca. 0.80 eV higher in energy than ${}^4\mathbf{1b}^+$. In this state the Fe–O1 and the Fe–O2 bonds are shorter and longer, respectively, than those of ${}^5\mathbf{1a}^{2+}$, but both are longer than those of ${}^3\mathbf{1a}^{2+}$. Comparison between the MO diagrams of ${}^4\mathbf{1a}^+$ and ${}^5\mathbf{1a}^{2+}$ (both have less severe spin contamination; S^2 for ${}^4\mathbf{1a}^+$ is 3.81, and the ideal value is 3.75) shows that the added electron goes into the $\text{O}(\text{p}_x, \text{p}_y)$ β -orbital, with the π interaction of Fe–O1 being bonding, but for Fe–O2 being antibonding in character. It is thus reasonable for the Fe–O1 and Fe–O2 bonds to be shorter and longer, respectively, than those of ${}^5\mathbf{1a}^{2+}$.

D. Electron affinities of $\mathbf{1}^{2+}$. The gas-phase adiabatic electron affinities (EA_{ad}) are in the range 9.32–9.53 eV, spanning a range of ca. 200 meV. With solvent, MeCN, included the EA_{ad} drops to 5.86–6.06 eV, with a similar redox poten-

tial window. In general, the quintet states have the highest electron affinities and the triplet states have the lowest electron affinities, irrespective of whether they are in the gas phase or in MeCN.

2. $[\text{Fe}(\text{O})_2(\text{tpy})]^{n+}$ (3)

A. Optimized geometries and relative energies of the different spin states of $\mathbf{3}^{2+}$. The optimized geometries and relative energies of $\mathbf{3}^{2+}$ in various spin states are listed in Table S3. There is only one minimum for each spin state, $S = 0$ and 1, with the triplet state being more stable than the singlet state by ca. 0.46 eV. The quintet state does not converge to any local minimum. The geometries are similar for both optimized singlet and triplet states, and are essentially TBP structures. The Fe–O bonds are short, ca. 1.586 Å, for both the optimized singlet and triplet states. The O–Fe–O angles for the two spin states, 119° for the triplet and 114° for the

singlet state, are similar. Contrary to $^{3,5}\mathbf{1b}^{2+}$ and $^{3,5}\mathbf{1c}^{2+}$, the O–Fe–O moiety is symmetrically disposed about the tpy plane, with O1–Fe–N2 angle being ca. 121 and 123° for the singlet and triplet states, respectively.

B. Electronic structures of the different spin states of 3^{2+} . The key MOs for 3^{2+} are depicted in Figure S1 in the Supporting Information. The lowest energy d-orbital involves the π -antibonding combination of the Fe(d_{xy}) and O(p_x) orbitals, the second lowest is given by a π^* -combination of the Fe(d_{xz}) and O(p_x) orbitals, similar to that found for $\mathbf{1}^{2+}$ with a TBP geometry (Figure 1). The third-lowest lying d-orbital involves the π -antibonding interaction of the Fe($d_{x^2-y^2}$, d_{z^2}) and O(p_y) orbitals, instead of involving the Fe(d_{yz} , $d_{x^2-y^2}$) orbital as in the case of $^{3,5}\mathbf{1c}^{2+}$. Moreover, both oxido ligands contribute equally to this MO in 3^{2+} , whereas the O2 ligand contributes more in the cases of $^{3,5}\mathbf{1c}^{2+}$ due to the asymmetrical disposition of the O–Fe–O moiety about the py1–py3 plane. The σ -antibonding combination of the Fe(d_{yz}) and O(p_z) orbitals is the second highest energy d-orbital, and the MO comprising the σ^* interaction of the Fe(d_{z^2} , $d_{x^2-y^2}$) and O(p_y , p_z) orbitals is highest in energy. For 3^{2+} there are no mixed σ^*/π^* interactions observed in the frontier orbitals as found for $^{3,5}\mathbf{1b}^{2+}$ and $^{3,5}\mathbf{1c}^{2+}$.

For $\mathbf{1}^{3^{2+}}$ the lowest-energy d_{xy} orbital is doubly occupied, leaving the other four d-orbitals unoccupied. Thus, $\mathbf{1}^{3^{2+}}$ could be described as $[\text{Fe}^{\text{VI}}(\text{O})_2(\text{tpy})]^{2+}$. For $^{3,5}\mathbf{1b}^{2+}$ and $^{3,5}\mathbf{1c}^{2+}$ the d_{xy} and d_{xz} orbitals are singly occupied and hence it could also be described as $[\text{Fe}^{\text{VI}}(\text{O})_2(\text{tpy})]^{2+}$. As both singlet and triplet states have electrons occupying orbitals with $\pi^*(\text{Fe–O})$ character, it is not surprising that both states have similar Fe–O bond lengths. The fact that the triplet state is more stable than the singlet state may be attributed to the electronic structure of the triplet state, which has two unpaired d-electrons and this extra d–d exchange interaction makes $^{3,5}\mathbf{1b}^{2+}$ more stable than the singlet state.

C. Optimized geometries, relative energies, and electronic structures of 3^+ in different spin states. There is also one minimum energy structure located for each of the doublet and quartet states, with the quartet state being more stable than the doublet state by ca. 0.45 eV. The Fe–O distances become longer upon one-electron reduction of $[\text{Fe}(\text{O})_2(\text{tpy})]^{2+}$: ca. 1.612 Å for the doublet state, and 1.600 and 1.617 Å for the quartet state. Noticeably, the O–Fe–O unit is symmetrically disposed about the tpy plane for the doublet state, as in $\mathbf{1}^{3^{2+}}$, however, it is asymmetrically disposed about the tpy plane for the quartet state: the N2–Fe–O1 angle is 145°, while the N2–Fe–O2 angle is 98° for $\mathbf{4}^{3+}$ (see Table S3 in the Supporting Information). Such asymmetric disposition of the O–Fe–O unit about the plane defined by the three pyridyl rings coordinated to the Fe has also been found for $^{3,5}\mathbf{1b}^{2+}$, $^{3,5}\mathbf{1c}^{2+}$, and $\mathbf{4}^{1b^{2+}}$.

Taking a look at the electronic structures of $^{2,4}\mathbf{3}^{+}$, the MO diagram of the doublet state is similar to that of the singlet or triplet state with two electrons doubly occupying the d_{xy} orbital and one electron singly occupying the d_{xz} orbital. Hence, $\mathbf{2}^{3+}$ can be described as $[\text{Fe}^{\text{V}}(\text{O})_2(\text{tpy})]^+$. Since there is one more electron occupying the $\pi^*(\text{Fe–O})$

orbital in the doublet state, the Fe–O bonds are longer than those in the singlet and triplet states. For the quartet state the MO compositions are different from the singlet and triplet states. The two lowest lying d-orbitals of $\mathbf{4}^{3+}$ are similar to those of the singlet, triplet, and doublet states. However, the three highest lying d-orbitals are derived from the π^* interaction between the Fe(d_{yz} , $d_{x^2-y^2}$) and O(p_y) orbitals, σ^*/π^* interaction between the Fe(d_{z^2} , $d_{x^2-y^2}$) and O(p_y , p_z) orbitals, and σ^*/π^* interaction between the Fe($d_{x^2-y^2}$, d_{yz}) and O(p_z) orbitals, respectively. Such MO compositions and interactions are similar to those of $^{3,5}\mathbf{1b}^{2+}$, $^{3,5}\mathbf{1c}^{2+}$, and $\mathbf{4}^{1b^{2+}}$. All these structures ($\mathbf{4}^{3+}$, $^{3,5}\mathbf{1b}^{2+}$, $^{3,5}\mathbf{1c}^{2+}$, and $\mathbf{4}^{1b^{2+}}$) have three unpaired electrons in the three lowest lying d-orbitals. Indeed, the quartet state calculated with the triplet state geometry of 3^{2+} [with O–Fe–O symmetrically disposed about the plane defined by Fe(tpy)] is less stable than the optimized quartet state by as much as 0.53 eV. Thus, a d^3 electronic configuration in TBP geometry may prefer an asymmetrical disposition of the O–Fe–O unit about the tpy plane. This preference may come from a decrease in the energy of the (d_{yz} , $d_{x^2-y^2}$) $\pi^*(\text{Fe–O})$ orbital in the asymmetrical geometry, such that the d–d exchange stabilization is more enhanced (the orbital energy is lowered from –7.495 eV for the triplet symmetrical optimized geometry to –8.600 eV for the quartet asymmetrical optimized geometry; the other two occupied d-orbitals are lowered by less than 0.27 eV). Nevertheless, $\mathbf{4}^{3+}$ could also be described as $[\text{Fe}^{\text{V}}(\text{O})_2(\text{tpy})]^+$.

D. Electron affinities of 3^{2+} . The gas phase EA_{ad} values are in the range 9.96–10.42 eV, spanning a range of ca. 460 meV. When the various states are placed in MeCN, the electron affinities decrease to span the range 5.71–6.19 eV.

3. *trans*- $[\text{Fe}(\text{O})_2(\text{NH}_3)_2(\text{NMeH}_2)_2]^{n+}$ (**2**)

We have previously reported calculations on $\mathbf{2}^{2+/+}$.^[15] However, in order to compare the results of **2** with those of **1** and **3**, we have redone the calculations using UOLYP/BS1.

A. Optimized geometries and relative energies of the different spin states of 2^{2+} . The optimized geometries and relative energies of 2^{2+} with $S = 0, 1$, and 2 are given in Table S5 in the Supporting Information. There is only one local minimum found for each spin state. As reported previously,^[15] the lowest energy state is the singlet, with the Fe–O distances being within the range 1.607–1.613 Å, and the O–Fe–O angle being essentially linear. The quintet state is the highest energy state (1.19 eV higher than $\mathbf{1}^{2^{2+}}$) with the longest Fe–O bonds (1.737–1.745 Å) amongst the three spin states, $S = 0, 1$, and 2, and with a O–Fe–O angle that deviates significantly from linearity (ca. 164°). These geometric features of $\mathbf{5}^{1^{2+}}$ have been reported previously.^[15] In this study we have also located a minimum for the triplet state. The Fe–O distances are between those observed for the singlet and quintet states, being within the range 1.652–

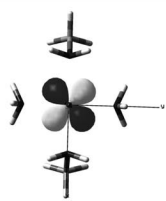













	dominant Fe(d_{xy})	dominant O(p_π)
Singlet	 MO43	 MO42
Triplet	 α -MO40	 α -MO42
	 β -MO41	 β -MO43
Quintet	 α -MO40	 α -MO42
	 β -MO43	 β -MO42
Quartet	 α -MO42	 α -MO40
	 β -MO41	 β -MO43

Figure 3. MO surfaces involving Fe(d_{xy}) and O(p_π) orbitals with the optimized geometries of 2^{n+} ($n = 2$ for singlet, triplet, and quintet states and $n = 1$ for the quartet state). The corresponding MO surfaces for the doublet state are similar to those for the singlet state.

1.688 Å. The O–Fe–O angle is also not linear in the triplet state, and is ca. 166°. The $^3\mathbf{2}^{2+}$ state lies 0.84 eV above the singlet state.

B. Electronic structures of $\mathbf{2}^{2+}$ in different spin states. The MO diagram of $\mathbf{1}^{2+}$ has been reported previously.^[15] Herein, we only briefly mention the key MOs. The lowest lying d-orbital is the nonbonding Fe(d_{xy}) orbital, the second lowest is created by a π^* combination between the Fe(d_{xz}, d_{yz}) and O(p_x, p_y) orbitals. The second highest lying d-orbital is derived from the σ^* interaction between the Fe($d_{x^2-y^2}$) and amine N(σ) orbitals. The highest lying orbital is attributed to the σ^* combination of the Fe(d_{z^2}) and O(p_z) orbitals. For the singlet state the d_{xy} orbital is doubly occupied leaving other d-orbitals empty. Thus, $\mathbf{1}^{2+}$ is described as *trans*-[Fe^{VI}(O)₂(NH₃)₂(NMeH₂)₂]²⁺.

For the triplet and quintet states the key orbitals are similar to those of the singlet state, except for the Fe(d_{xy}) orbital and the nonbonding O(p_x, p_y) orbitals. As the O–Fe–O angle is bent in both the triplet and quintet states, the Fe(d_{xy}) orbital is no longer nonbonding as in the singlet state, but has some π interactions with the nonbonding O(p_π) pair (see Figure 3 for the MO surfaces of these orbitals for the singlet, triplet, and quintet states). In the triplet state the orbital with dominant d_{xy} character (α -MO40 and β -MO41) is doubly occupied but the O(p_y) orbital, which is mixed with a significant amount of Fe(d_{xy}) character, is singly occupied (α -MO42 is filled, but β -MO43 is vacant). The other α -electron occupies the $\pi^*(\text{Fe–O})$ orbital. As such, $^3\mathbf{2}^{2+}$ has two resonance structures: [Fe^{VI}(O)₂]²⁺ \leftrightarrow [Fe^V(O)₂]²⁺. For the quintet state the orbitals with dominant Fe(d_{xy}) and O(p_π) characters are both singly occupied (α -MO40 and α -MO42 are filled, but β -MO42 and β -MO43 are empty). The $\pi^*(\text{Fe–O})$ orbitals are also singly occupied. Thus, there are a total of three unpaired electrons on Fe and one unpaired electron on the oxido ligands. Hence, the formulation of $^5\mathbf{2}^{2+}$ is described as *trans*-[Fe^V(NH₃)₂(NMeH₂)₂(O)₂]²⁺.

C. Optimized geometries, relative energies, and electronic structures of the different spin states of $\mathbf{2}^+$. We have found one minimum energy structure for each of the doublet and quartet states, with the latter state ca. 0.53 eV higher in energy than the former state. Compared with the singlet state, the doublet state has longer Fe–O bond lengths (1.668–1.686 Å) that are comparable to those found for the triplet state. The O–Fe–O angle of the doublet state is essentially linear, as in the singlet state. For the quartet state the Fe–O distances are longer than those of the triplet state, but comparable to those of the quintet state (1.736–1.775 Å). The O–Fe–O angle is only slightly bent (ca. 173°) in the quartet state. These results are in good agreement with those obtained in a previous study.^[15]

For the doublet state, the extra electron is added to the $\pi^*(\text{Fe–O})$ orbital of the singlet state. Thus, the Fe–O bonds are elongated, and $^2\mathbf{2}^+$ could be formulated as *trans*-[Fe^V(O)₂(NH₃)₂(NMeH₂)₂]⁺.

For the quartet state, as the O–Fe–O angle is slightly bent from linearity, there is mixing between the Fe(d_{xy}) and O(p_y) orbitals, though to a lesser extent compared to the

case of $^3,^5\mathbf{2}^{2+}$. The orbital with dominant Fe(d_{xy}) character is doubly occupied, while the one with dominant O(p_y) character is singly occupied (i. e., α -MO40, α -MO42, and β -MO41 are occupied, but β -MO43 is unoccupied; see Figure 3 for the MO surfaces). The other two electrons each singly occupy the $\pi^*(\text{Fe–O})$ orbitals. Thus, as for $^3\mathbf{2}^{2+}$, there are two resonance forms for $^4\mathbf{2}^+$: [Fe^V(O)₂]⁺ \leftrightarrow [Fe^{IV}(O)₂]²⁺, with the [Fe^V(O)₂]⁺ structure being prevalent.

D. Electron affinities of $\mathbf{2}^{2+}$. The gas phase EA_{ad} values were calculated to be 10.77–11.43 eV, a redox potential window of ca. 660 meV. With solvent, MeCN, included the electron affinities decrease to 5.50–5.89 eV with a concomitant drop in the range to ca. 400 meV, contrary to the cases for both $\mathbf{1}^{2+}$ and $\mathbf{3}^{2+}$ where the solvent does not alter the redox potential range.

Discussions

A. TBP vs. PBP structures of [Fe(O)₂(qpy)]²⁺. Geometry optimizations with the functional OLYP predict that the TBP structure is more stable than the PBP structure by at least 0.7 eV. This may be due to the stronger Fe–O bonding in the TBP structure compared to the PBP structure, as reflected by the former having a shorter Fe–O bond length and higher Wiberg Bond Indices (WBI) than the latter [WBI values, which are correlated to the bond order, for the $^3(^5)\mathbf{1a}^{2+}$ PBP structure are 1.26 (0.88) and 0.87 (0.72) for the Fe–O1 and Fe–O2 bonds, respectively; and for the $^3(^5)\mathbf{1c}^{2+}$ TBP structure they are 1.24 (1.23) and 1.20 (1.17) for the Fe–O1 and Fe–O2 bonds, respectively]. However, as mentioned above, $^5\mathbf{1a}^{2+}$ is predicted to be the most stable structure according to the B3LYP functional calculations. High-level ab initio calculations would thus be valuable for determining the relative energies of these two structures.

Do the two different coordination geometries calculated for $\mathbf{1}^{2+}$ influence the mechanisms by which this complex undergoes reactions? Let us first take a look at the lowest unoccupied orbital of the transition metal complex with oxido contributions. This unoccupied orbital acts as an acceptor orbital in the oxygen atom transfer reaction and overlaps with the substrate donor orbital, such as $\phi_{\text{C=C}}$ in epoxidation reactions and ϕ_{CH} in hydroxylation reactions. The lower the energy and the larger the oxido character of this unoccupied orbital of the transition metal complex is, the better the complex would be as an oxidant, and the lower the activation energy will be for C=C or C–H oxidation, based on the energetics of these ground state orbitals. For the seven-coordinate $^5\mathbf{1a}^{2+}$ with PBP structure, both the α and β -LUMOs have significant oxido character [64% O1(p_π) character for α -LUMO and 34% O2(p_π) character for β -LUMO] and are quasi-degenerate. For $^3\mathbf{1c}^{2+}$ the lowest unoccupied orbital is the β -LUMO that lies ca. 1.2 eV above the corresponding orbital of $^5\mathbf{1a}^{2+}$ (see Table S2 in the Supporting Information) and have only ca. 16% and 11% O1 and O2 character, respectively. The α -LUMOs of $^5\mathbf{1c}^{2+}$ lie even higher in energy, ca. 2 eV above those of $^5\mathbf{1a}^{2+}$.

and have substantially less oxido character, with ca. 14% O1 and 8% O2 orbital contributions. As such, based on MO energies and the oxido contributions of the accepting orbitals of the different geometries of 1^{2+} , ${}^{3,5}\text{1a}^{2+}$ should act as a better oxido-transfer reagent than ${}^{3,5}\text{1c}^{2+}$. A similar trend is also expected when solvent is taken into account.

However, from the OLYP calculations, ${}^{5}\text{1a}^{2+}$ is substantially higher in energy than ${}^{3,5}\text{1b}^{2+}$ and ${}^{3,5}\text{1c}^{2+}$ by ca. 0.98 eV when in the gas phase and by 0.84 eV when in MeCN. However, it should be noted that it may be possible to generate 1a^{2+} from high spin $[\text{Fe}^{\text{II}}(\text{qpy})]^{2+}$ depending on the oxidant used. Mechanistic calculations would thus be valuable for deciphering whether such a reaction is viable.

B. Influence of the different spectator ligand L on the properties of $[\text{Fe}(\text{O})_2(\text{L})]^{2+}$. Are any of the high-valent dioxido-iron complexes studied in the present work superior to other compounds for catalyzing oxygenation reactions? Does solvent play any role? We will try to address these points based on the LUMO energies and EA_{ad} values (which are correlated with the reduction potential) of $1^{2+} - 3^{2+}$. Our discussion will mainly be focused on the lowest energy states, i.e. the ${}^{3,5}\text{1c}^{2+}$ (as they are close in energy, being within ca. 0.2 eV of each other), 1^{2+} , and ${}^{3,3^{2+}}$ states.

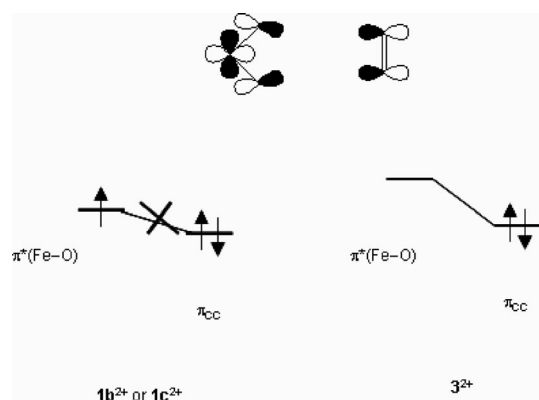
1. LUMOs and electron affinities. First, let us take a look at the accepting orbital(s) of the different complexes studied herein. The larger the oxido character and the lower the energy of this acceptor orbital is, the better the overlap between the substrate donor orbital and the complex acceptor orbital is. The oxido character of the accepting orbitals of ${}^{3}\text{1c}^{2+}$, 1^{2+} and ${}^{3,3^{2+}}$ are ca. 10–16%, 24%, and 9–17%, respectively. As shown in Tables S2, S4, and S6, the energies of the acceptor orbitals (LUMOs with oxido character) of the states in the gas phase are in the order: 1^{2+} (LUMO: -13.687 eV) < ${}^{3,3^{2+}}$ (α -LUMO: -12.264 eV; β -LUMO: -12.700 eV) < ${}^{3}\text{1c}^{2+}$ (α -LUMO: -10.953 eV; β -LUMO: -10.003 eV) < ${}^{5}\text{1c}^{2+}$ (α -LUMO: -9.301 eV; β -LUMO: -11.334 eV). Hence, 1^{2+} should have the most effective overlap with the substrate donor orbital and thus the lowest activation barrier for oxygen atom transfer reactions in the gas phase.^[22] A similar order of MOs was found when solvent (MeCN) effects were taken into account, except in the case of ${}^{5}\text{1c}^{2+}$ where the β -LUMOs are comparable in energy to the LUMO of 1^{2+} ; the LUMO energies of the states in MeCN are in the order: 1^{2+} (LUMO: -6.388 eV) < ${}^{3,3^{2+}}$ (α -LUMO: -6.282 eV; β -LUMO: -6.340 eV) < ${}^{5}\text{1c}^{2+}$ (α -LUMO: -4.637 eV; β -LUMO: -6.334 eV) < ${}^{3}\text{1c}^{2+}$ (α -LUMO: -6.177 eV; β -LUMO: -5.311 eV). Indeed, this is in concordance with the EA_{ad} values in the gas phase where 1^{2+} has the highest EA_{ad} (10.77 eV) and both the ${}^{3,5}\text{1b}^{2+}$ states have the lowest EA_{ad} values (9.32 and 9.41 eV for the triplet and quintet states, respectively). We have not computed the EA_{ad} of ${}^{3,5}\text{1c}^{2+}$ states, as their py4 and py5 orientations are different from that of ${}^4\text{1b}^{2+}$. Moreover, as the ${}^{3,5}\text{1c}^{2+}$ states are lower in energy than the corresponding spin states of 1b^{2+} the EA_{ad} values estimated for ${}^{3,5}\text{1c}^{2+}$ should be even smaller than those for ${}^{3,5}\text{1b}^{2+}$. However, in MeCN, ${}^{3,3^{2+}}$ and ${}^5\text{1b}^{2+}$ have the highest EA_{ad} values

(6.05 eV for the former and 6.06 eV for the latter), with the second highest being ${}^3\text{1b}^{2+}$ (5.88 eV), and 1^{2+} has the lowest EA_{ad} . Hence, changing the polarity of the solvent may induce a change in the redox behavior of the three complexes studied. Why are such solvent effects observed? When MeCN is included in the DFT calculation with a polarizable continuum model (PCM), the electronic states of 1^{2+} are shown to be stabilized by ca. 5.59–5.75 eV, while the 1^{+} states are stabilized by ca. 2.08–2.37 eV, irrespective of the coordination geometry of the complex. The solvent stabilization is substantial for 2^{2+} , ca. 8.09–8.42 eV, but MeCN stabilizes the states of 2^{+} by ca. 2.82–2.87 eV, which is comparable to the level of solvent stabilization experienced by the electronic states of 1^{+} . The states of 3^{2+} also have a larger solvent stabilization than those of 1^{2+} , but not as much as those of 2^{2+} , being ca. 6.52–6.54 eV, while the states of 3^{+} are stabilized by a similar amount as the states of 1^{+} and 2^{+} , ca. 2.18–2.30 eV.

Solvent effects are usually explained in terms of the dipole moment and polarizability of the complex. However, it seems that such an explanation could not be applied to the present results. First of all, irrespective of the spin states and coordination geometries (either TBP or PBP) of 1^{2+} where the dipole moment varies from 1.4192 D for ${}^3\text{1a}^{2+}$ to 19.6301 D for ${}^5\text{1c}^{2+}$, the solvent stabilizations are similar. Furthermore, 1^{2+} , being a highly symmetric structure, has the smallest dipole moment (1.925 D) and should thus have the smallest solvent stabilization amongst the complexes studied in this work. However, as described above, the stabilization of 1^{2+} is the largest amongst all the states for the complexes $1^{2+} - 3^{2+}$. Secondly, states ${}^{3,5}\text{1b}^{2+}$ and ${}^{3,5}\text{1c}^{2+}$, all of which have a qpy cation radical, should be the easiest to polarize, and hence have large polarizability values. Thus, these species should have the largest solvent stabilizations, but 1^{2+} is the least stabilized by MeCN. So why is 1^{2+} the least stabilized and 2^{2+} the most stabilized by MeCN? As the magnitude of solvent stabilization is a function of the spectator ligand, we envisioned that this unusual effect is a result of the nature of the spectator ligands. Simple amines, NH_3 and NMeH_2 , are stronger bases than pyridines. Thus, the electron densities on the N atoms are higher with amine ligands (as in **2**) than ligands with pyridyl rings (as in **1** and **3**). The NBO charges confirmed that this is the case: -0.26 to -0.51 for N1–N5 in 1^{2+} ; -0.41 to -0.43 for N1–N3 in 3^{2+} ; -0.77 to -1.00 for N1–N4 in 2^{2+} . Thus, this solvent effect arises from a classical electrostatic effect: the higher the charge, the stronger the stabilization will be. Complex 3^{2+} , though having slightly lower charge densities on its nitrogen atoms than calculated for those of 1^{2+} , has a slightly larger solvent stabilization than 1^{2+} . This may be explained by the shorter Fe–N distances in 3^{2+} than in 1^{2+} (see Tables S1 and S3 in the Supporting Information), leading to the slightly larger solvent stabilization of 3^{2+} with respect to 1^{2+} . As the monocationic ion has a smaller overall charge compared to the dicationic ion, the solvent stabilization is less pronounced. Thus, a reverse trend in electron affinity (and hence the reduction potential) order was found when these three complexes are placed in a polar solvent.

2. Implications to $[\text{Fe}(\text{O})_2(\text{L})]^{n+}$ Reactivity

As complexes 1c^{2+} and 3^{2+} have the oxido ligands bound in a *cis*-fashion, they may undergo alkene *cis*-1,2-dihydroxylation. However, in the electronic structures of 1b^{2+} and 1c^{2+} the π^* orbital (d_{yz}), which can overlap with the $\text{C}=\text{C}$ π -orbital, is singly occupied in both the triplet and quintet states (see Figure 1). The Woodward–Hoffmann $4n+2$ rule tells us that this interaction, which involves three electrons, is unfavourable (see Scheme 3). On the other hand, 3^{2+} has a vacant π^* -orbital ($d_{x^2-y^2}, d_{z^2}$) that can interact with the alkene $\text{C}=\text{C}$ π -bond and this interaction will involve only two electrons. Indeed, we have not been able to obtain *cis*-diol products from the reactions of electron-deficient alkenes with Oxone when $[\text{Fe}(\text{qpy})]^{2+}$ is employed as a catalyst.



Scheme 3.

Conclusions

In this work we have employed DFT to study $[\text{Fe}(\text{O})_2(\text{L})]^{2+}$, with $\text{L} = \text{qpy}$, simple amines, and *tpy*, in order to see how the coordination number of the spectator ligand L affects the electronic structure and hence the reactivity of these oxido-iron complexes. It was found that *qpy*, though a pentadentate ligand in $[\text{Fe}^{\text{II}}(\text{qpy})(\text{NCMe})_2]^{2+}$, can adopt two geometries when the two acetonitrile ligands are replaced by two oxido ligands, and these two geometries are TBP and PBP. In the former, *qpy* acts as a tridentate ligand with the oxido ligands positioned in a *cis* fashion; in the latter case, *qpy* acts as a pentadentate ligand with the oxido ligands *trans* to each other. Such differences in the coordination geometries have a significant impact on the electronic structures of **1**. With TBP geometry (1b^{2+} or 1c^{2+}), **1** adopts a $[\text{Fe}^{\text{V}}(\text{O})_2(\text{qpy})^+]^{2+}$ formalism and the electronic structure resembles that of heme Cpd I: a d^3 quartet Fe ion ferromagnetically and antiferromagnetically coupled to the *qpy* cation radical in 1b^{2+} and 1c^{2+} to give the quintet and triplet states, respectively (Cpd I has the d^4 triplet ferromagnetically and antiferromagnetically coupled to a porphyrin cation radical to give doublet and quartet states, respectively).^[21] Thus, it is likely that 1^{2+} in a TBP geometry will display similar reactivity properties as heme Cpd I. With a PBP geometry (51a^{2+}) the acceptor orbitals, $\pi^*(\text{Fe}-\text{O})$, are

at least 200 meV lower in energy than those for the TBP geometry. In addition, the oxido character is more localized and contributes more to the acceptor orbital of 1^{2+} with PBP geometry (1a^{2+}) than with TBP geometry (1b^{2+} and 1c^{2+}), such that oxygen atom transfer reactions may be more efficient in the former case than in the latter case.

With variation in the coordination number, dioxido-iron complexes can change from a high-spin triplet with $\text{L} = \text{tridentate tpy}$ to a low-spin singlet with $\text{L} = \text{amines occupying the four equatorial positions}$, and to quasi-degenerate triplet and quintet state with $\text{L} = \text{qpy}$. The former two complexes could be described as $[\text{Fe}^{\text{VI}}(\text{O})_2]^{2+}$, whereas the latter as $[\text{Fe}^{\text{V}}(\text{O})_2(\text{qpy})^+]^{2+}$ with a TBP geometry. The electron affinity was found to follow the order $1^{2+} > 3^{2+} > {}^{3,5}1\text{b}^{2+}$ in the gas phase, but 1^{2+} is slightly more difficult to reduce in MeCN than 3^{2+} and ${}^{3,5}1\text{b}^{2+}$.

Computational Details

Herein, we studied $[\text{Fe}(\text{O})_2(\text{L})]^{n+}$ with L having different coordination numbers: (1) $\text{L} = \text{qpy}$, which can at most have 5 coordination sites; (2) $\text{L} = \text{simple amines } \text{NH}_3 \text{ and } \text{NMe}_2 \text{ occupying the equatorial positions}$; and (3) *tpy*, where the ligand has three coordination sites. Spin states of $S = 0, 1$, and 2 for $n = 2$, and $S = 1/2$ and $3/2$ for $n = 1$ have been considered for all three complexes.

All calculations were performed with the G03 suite of programs^[23] with the density functional OLYP,^[24,25] which has been found to be reliable in reproducing relative spin-state energetics of complexes containing iron and ligands with different ligand field strengths.^[26] Unrestricted formalism was applied for all calculations involving the singlet states. For the geometry optimizations and subsequent frequency calculations the following basis sets, denoted as BS1, were used: 6-31G* for C and H atoms, 6-31+G* for N and O atoms,^[27–29] and Stuttgart relativistic pseudopotentials and its accompanying basis set for Fe.^[30,31] As no imaginary frequencies were found, all optimized geometries for the different spin states were found to be at true local energy minima. The wavefunctions were also found to be stable after stability test.

Solvent effects were included with PCM as implemented in G03.^[23] Herein, we used the solvent, MeCN, as most of the experimental reactions involving the nonheme iron-oxido complexes were carried out in this solvent, and the oxidation reactions with Oxone catalysed by $[\text{Fe}(\text{qpy})(\text{MeCN})_2]^{2+}$ were performed in MeCN.

Single-point energy calculations with a larger basis set (BS2) have also been employed: 6-311G* for all non-Fe atoms^[32] and the same pseudopotential and basis sets as BS1 for Fe. It was found that the relative spin state energetics computed using UOLYP/BS2 are essentially the same as those calculated with UOLYP/BS1. Single-point energy calculations with a hybrid density functional B3LYP,^[25,33,34] have also been performed with the large BS2 basis set.

Supporting Information (see also the footnote on the first page of this article). Optimized geometries, frontier orbital energies, electron affinities, spin densities, and MO diagrams for **1–3** are given in the Supporting Information.

Acknowledgments

This work was supported by the University Grants Council (HKU 700906) and the University Grants Committee of Hong Kong,

SAR of China (Area of Excellence Scheme AoE/P1-0/01). C.-M. C. would like to thank the University Development Fund of the University of Hong Kong for financial support. The authors also thank the Computer Center at the University of Hong Kong for providing supercomputer time.

- [1] M. Sono, M. P. Roach, E. D. Coulter, J. H. Dawson, *Chem. Rev.* **1996**, 96, 2841.
- [2] E. I. Solomon, T. C. Brunold, M. I. Davis, J. N. Kemsley, S.-K. Lee, N. Lehnert, F. Neese, A. J. Skulan, Y.-S. Yang, J. Zhou, *Chem. Rev.* **2000**, 100, 235.
- [3] B. Meunier, S. P. de Visser, S. Shaik, *Chem. Rev.* **2004**, 104, 3947.
- [4] S. V. Kryatov, E. V. Rybak-Akimova, S. Schindler, *Chem. Rev.* **2005**, 105, 2175.
- [5] M. Costas, M. P. Mehn, M. P. Jensen, L. Que Jr., *Chem. Rev.* **2004**, 104, 939.
- [6] J. T. Groves, *J. Inorg. Biochem.* **2006**, 100, 434.
- [7] C. Krebs, D. G. Fujimori, C. T. Walsh, J. M. J. Bollinger, *Acc. Chem. Res.* **2007**, 40, 484.
- [8] S. S. Gupta, M. Stadler, C. A. Noser, A. Ghosh, B. Steinhoff, D. Lenoir, C. P. Horwitz, K.-W. Schramm, T. J. Collins, *Science* **2002**, 296, 326.
- [9] A. Chanda, D.-L. Popescu, F. Tiago de Oliveira, E. L. Bominaar, A. D. Ryabov, E. Muenck, T. J. Collins, *J. Inorg. Biochem.* **2006**, 100, 606.
- [10] D. N. Harischandra, G. Lowery, R. Zhang, M. Newcomb, *Org. Lett.* **2009**, 11, 2089.
- [11] W. Nam, *Acc. Chem. Res.* **2007**, 40, 522.
- [12] X. Shan, L. Que Jr., *J. Inorg. Biochem.* **2006**, 100, 421.
- [13] S. Sinnecker, N. Svensen, E. W. Barr, S. Ye, J. M. Bollinger Jr., F. Neese, C. Krebs, *J. Am. Chem. Soc.* **2007**, 129, 6168.
- [14] F. Tiago de Oliveira, A. Chanda, D. Banerjee, X. Shan, S. Mondal, L. Que Jr., E. L. Bominaar, E. Muenck, T. J. Collins, *Science* **2007**, 315, 835.
- [15] G. S. M. Tong, E. L.-M. Wong, C.-M. Che, *Chem. Eur. J.* **2008**, 14, 5495.
- [16] For experimental details please see the Supporting Information.
- [17] P. Liu, E. L.-M. Wong, A. W.-H. Wong, C.-M. Che, *Org. Lett.* **2008**, 10, 3275.
- [18] K. Roy, J. England, A. T. Fiedler, M. Martinho, E. Muenck, L. Que Jr., *Angew. Chem. Int. Ed.* **2008**, 47, 8068.
- [19] E. L.-M. Wong, G.-S. Fang, C.-M. Che, N. Zhu, *Chem. Commun.* **2005**, 4578.
- [20] A. Ghosh, *J. Inorg. Biochem.* **2006**, 100, 419.
- [21] S. Shaik, H. Hirao, D. Kumar, *Acc. Chem. Res.* **2007**, 40, 532.
- [22] C. Michel, E. J. Baerends, *Inorg. Chem.* **2009**, 48, 3628.
- [23] M. J. Frisch, G. W. Trucks, H. B. Schlegel, G. E. Scuseria, M. A. Robb, J. R. Cheeseman, J. J. A. Montgomery, T. Vreven, K. N. Kudin, J. C. Burant, J. M. Millam, S. S. Iyengar, J. Tomasi, V. Barone, B. Mennucci, M. Cossi, G. Scalmani, N. Rega, G. A. Petersson, H. Nakatsuji, M. Hada, M. Ehara, K. Toyota, R. Fukuda, J. Hasegawa, M. Ishida, T. Nakajima, Y. Honda, O. Kitao, H. Nakai, M. Klene, X. Li, J. E. Knox, H. P. Hratchian, J. B. Cross, V. Bakken, C. Adamo, J. Jaramillo, R. Gomperts, R. E. Stratmann, O. Yazyev, A. J. Austin, R. Cammi, C. Pomelli, J. W. Ochterski, P. Y. Ayala, K. Morokuma, G. A. Voth, P. Salvador, J. J. Dannenberg, V. G. Zakrzewski, S. Dapprich, A. D. Daniels, M. C. Strain, O. Farkas, D. K. Malick, A. D. Rabuck, K. Raghavachari, J. B. Foresman, J. V. Ortiz, Q. Cui, A. G. Baboul, S. Clifford, J. Cioslowski, B. B. Stefanov, G. Liu, A. Liashenko, P. Piskorz, I. Komaromi, R. L. Martin, D. J. Fox, T. Keith, M. A. Al-Laham, C. Y. Peng, A. Nanayakkara, M. Challacombe, P. M. W. Gill, B. Johnson, W. Chen, M. W. Wong, C. Gonzalez, J. A. Pople, *Gaussian 03*, rev. E.05, C. T. Wallingford, **2004**.
- [24] N. C. Handy, A. J. Cohen, *Mol. Phys.* **2001**, 99, 403.
- [25] C. Lee, W. Yang, R. G. Parr, *Phys. Rev. B* **1988**, 37, 785.
- [26] G. Ganzenmuller, N. Berkaine, A. Fouqueau, M. E. Casida, M. Reiher, *J. Chem. Phys.* **2005**, 122, 234321/1.
- [27] P. C. Hariharan, J. A. Pople, *Theor. Chim. Acta* **1973**, 28, 213.
- [28] W. J. Hehre, R. Ditchfield, J. A. Pople, *J. Chem. Phys.* **1972**, 56, 2257.
- [29] T. Clark, J. Chandrasekhar, G. W. Spitznagel, P. v. R. Schleyer, *J. Comput. Chem.* **1983**, 4, 294.
- [30] D. Andrae, U. Haeussermann, M. Dolg, H. Stoll, H. Preuss, *Theor. Chim. Acta* **1990**, 77, 123.
- [31] M. Dolg, U. Wedig, H. Stoll, H. Preuss, *J. Chem. Phys.* **1987**, 86, 866.
- [32] R. Krishnan, J. S. Binkley, R. Seeger, J. A. Pople, *J. Chem. Phys.* **1980**, 72, 650.
- [33] A. D. Becke, *J. Chem. Phys.* **1993**, 98, 1372.
- [34] P. J. Stephens, F. J. Devlin, C. F. Chabalowski, M. J. Frisch, *J. Chem. Phys.* **1994**, 98, 11623.

Received: June 15, 2010

Published Online: October 4, 2010